

## Supporting Information

### **Synthesis and investigation of mechanism of platinum-graphene electrocatalysts by novel co-reduction techniques for proton exchange membrane fuel cell applications**

*B. P. Vinayan, Rupali Nagar, and S. Ramaprabhu\**

Alternative Energy and Nanotechnology Laboratory (AENL), Nano Functional Materials  
Technology Centre (NFMTC),

Department of Physics, Indian Institute of Technology Madras, Chennai 600 036, India

Phone: + 91- 44- 22574862, Fax: +91- 44 - 22570509/22574852;

Corresponding author email: [ramp@iitm.ac.in](mailto:ramp@iitm.ac.in)

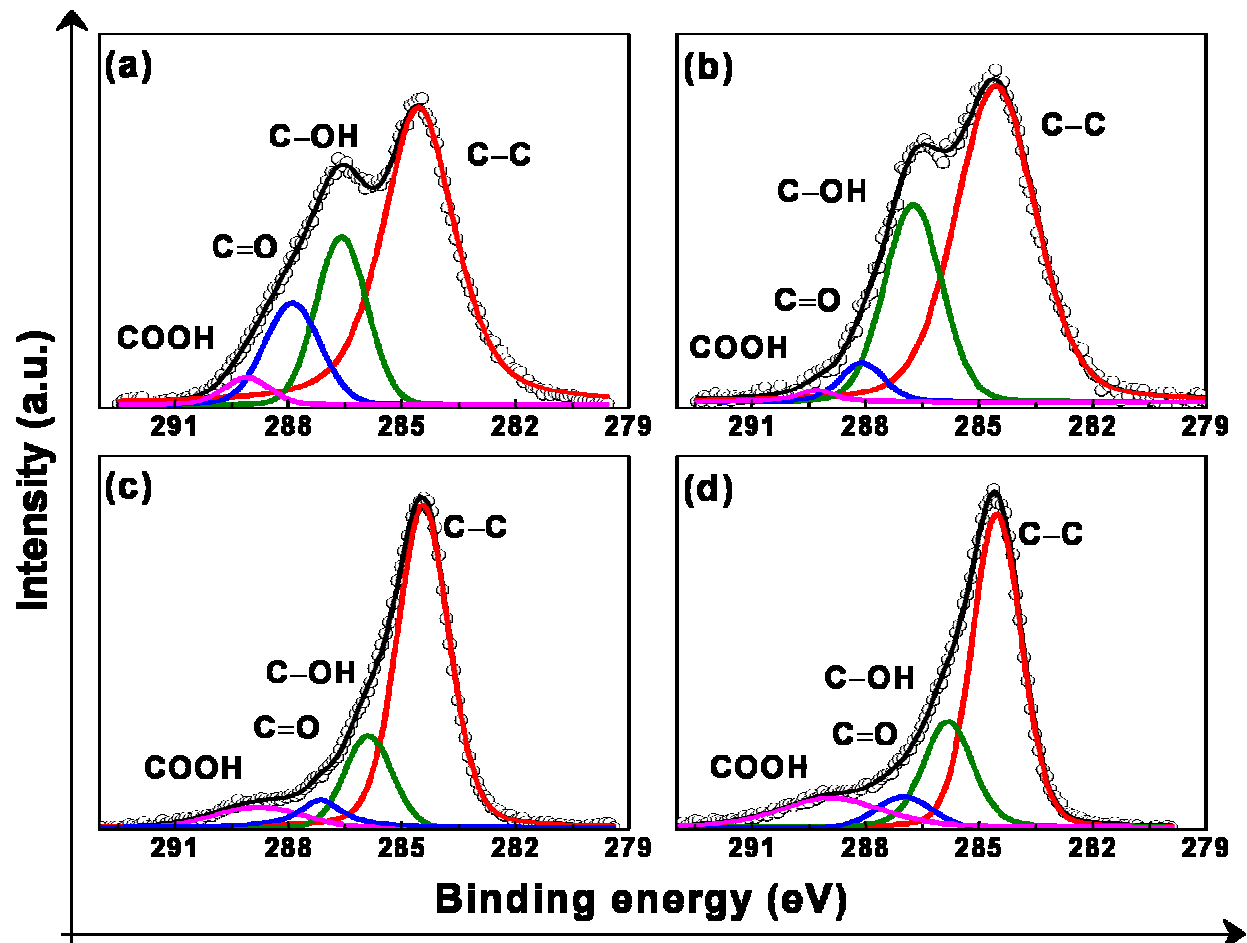
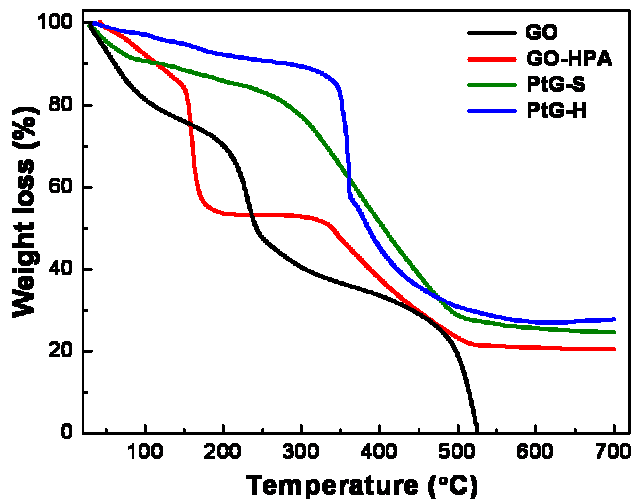


Fig. S1: XPS core level spectra corresponding to C1s orbital for (a) GO (b) GO-HPA, (c) PtG-S, and (d) PtG-H.

**Table S1:** Peak positions of deconvoluted C1s and Pt 4f XPS spectra.

Sample	Peak positions	
	C1s (eV)	Pt 4f (eV)
GO	284.56 [-C-C] 286.60 [-C-OH] 287.90 [-C=O] 289.10 [-COOH]	
GO-HPA	284.57 [-C-C] 286.76 [-C-OH] 288.10 [-C=O] 289.30 [-COOH]	73.56 & 77.96 (Pt <sup>+2</sup> ) 75.41 & 79.03 (Pt <sup>+4</sup> )
PtG-S	284.56 [-C-C] 285.90 [-C-OH] 287.15 [-C=O] 288.79 [-COOH]	71.29 (Pt <sup>0</sup> <sub>7/2</sub> ) 74.64 (Pt <sup>0</sup> <sub>5/2</sub> ) 73.08 (Pt <sup>+2</sup> <sub>7/2</sub> ) 76.37 (Pt <sup>+2</sup> <sub>5/2</sub> )
PtG-H	284.56 [-C-C] 285.83 [-C-OH] 287.00 [-C=O] 288.90 [-COOH]	71.44 (Pt <sup>0</sup> <sub>7/2</sub> ) 74.63 (Pt <sup>0</sup> <sub>5/2</sub> ) 72.70 (Pt <sup>+2</sup> <sub>7/2</sub> ) 75.90 (Pt <sup>+2</sup> <sub>5/2</sub> )

Fig. S2. shows the thermogravimetric analysis (TGA) of (a) GO, (b) GO-HPA, (c) PtG-S, and (d) PtG-H in air atmosphere at a heating rate  $20\text{ }^{\circ}\text{C min}^{-1}$ . The TGA curve of GO and GO-HPA shows a gradual mass loss till  $150\text{ }^{\circ}\text{C}$  due to the removal of moisture present in the sample. TGA shows that the temperature at which oxygen containing functional groups are removed from pure GO is at around  $200\text{ }^{\circ}\text{C}$ , but in GO-HPA the oxygen contents are removed even at lower temperature  $\sim 160\text{ }^{\circ}\text{C}$ . This may be due to the presence of Pt complexes within GO-HPA composite can catalyze the reduction of GO. In the same temperature range, the weight loss is negligible for PtG-S and PtG-H specimens suggesting a lesser moisture content in the specimens as compared to GO-HPA. A higher weight loss in case of PtG-S as compared to PtG-H up to  $200\text{ }^{\circ}\text{C}$  temperature indicates the increased amount of functional groups in the solar exfoliated sample. The weight loss of GO-HPA in the temperature range  $300\text{-}500\text{ }^{\circ}\text{C}$  is due to the oxidation of carbon and some removal of chlorine from the HPA. In this temperature range the weight loss in case of PtG-S and PtG-H is mainly due to carbon oxidation. Above  $525\text{ }^{\circ}\text{C}$  all graphene is completely burned to  $\text{CO}_2$  and only residual Pt is left within the samples. For GO-HPA the Pt content is 22 wt%, which confirms the removal of chlorine from HPA at high temperature by heat energy and conversion of Pt. Schweizer *et. al* have reported that the amount of Pt "missing" in the TGA experiment of HPA has been observed to vary with sample size, heating rate, and gas flow rate.<sup>1</sup> In PtG-S and PtG-H, the residual Pt content is 27 wt% and 29 wt%, respectively which confirms that majority of the HPA is converted to Pt by solar and hydrogen exfoliation.



**Fig. S2.** TGA of (a) GO, (b) GO-HPA, (c) PtG-S, and (d) PtG-H in air atmosphere at a heating rate  $20\text{ }^{\circ}\text{C min}^{-1}$ .

Fig. S3 presents the powder X-ray diffractograms of (a) graphite (Gr), (b) GO, (c) GO-HPA (d) solar exfoliated graphene (G-S) and (e) hydrogen exfoliated graphene (G-H), respectively. An intense crystalline peak occurs at a  $2\theta$  value of  $26.73^{\circ}$ , which is the characteristic peak of the (002) plane in hexagonal graphite with a  $d$ -spacing of 0.34 nm. Upon oxidation, the peak shifts to  $10.54^{\circ}$  as seen in Fig. S3(b), which corresponds to the (002) plane of graphite oxide. An increase in the interlayer spacing to 0.84 nm has been observed. This increase in  $d$ -spacing is due to the intercalation of  $-\text{OH}$  containing functional groups in between the graphene layers. The additional peaks in the XRD of GO at  $20.75^{\circ}$ ,  $26.73^{\circ}$ ,  $42.59^{\circ}$ , and  $77.6^{\circ}$  indicates that the GO is incompletely oxidized.<sup>2</sup> After exfoliation of GO with solar radiation at  $300\text{ }^{\circ}\text{C}$  and hydrogen at  $\sim 200\text{ }^{\circ}\text{C}$ , the  $10.54^{\circ}$  peak disappears and a broad peak ranging from  $14^{\circ}$  to  $30^{\circ}$  appears (Fig. S3(d) and S3(e)). This broad peak is suggestive of a loss of the long range order in the stacked layers of graphene. The interlayer spacing decreases to 0.37 nm for G-H and 0.36 for G-S, which suggests the removal of oxygen and water from the layers during exfoliation. The

interlayer spacing of exfoliated graphene is higher than the starting graphite powder (0.34 nm) suggesting loosening of graphene layers along the *c*-axis.

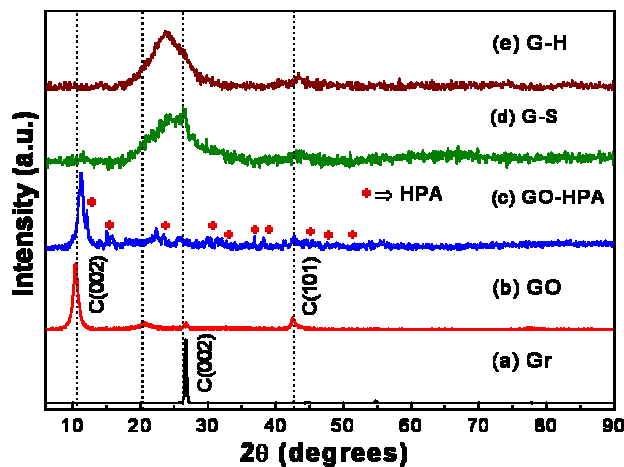


Fig. S3. X-ray diffractograms of (a) Gr, (b) GO, (c) GO-HPA, (d) G-S, and (e) G-H.

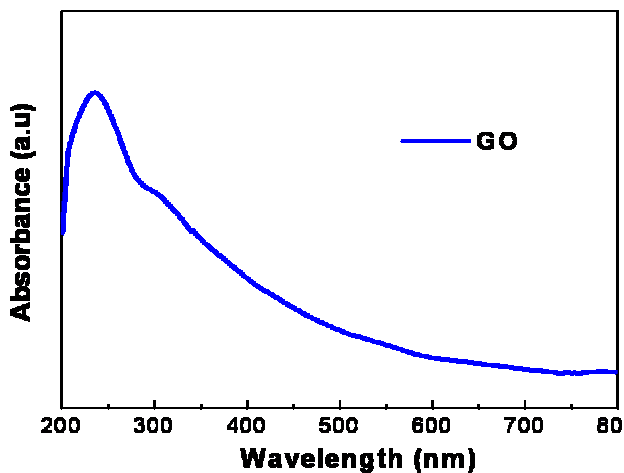
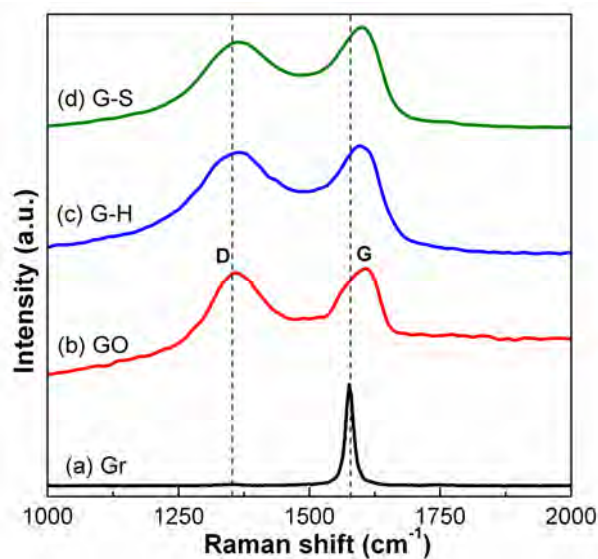


Fig. S4 : UV-Visible absorption spectra of GO

Fig. S5 represents the Raman spectra of (a) Gr, (b) GO and (c) G-S and (d) G-H. The absence of D-band in graphite shows that initial graphite used was defect free. Analogous to the optically allowed  $E_{2g}$  phonons at the brillouin zone center, a highly intense G band, occurs at  $\sim 1576.2 \text{ cm}^{-1}$ .<sup>1,3</sup> The G band of GO is present at  $1612 \text{ cm}^{-1}$ , but for G-S and G-H it shifts back to  $1596 \text{ cm}^{-1}$  and  $1592 \text{ cm}^{-1}$  respectively, towards the value of pristine graphite indicating the reduction of GO during solar exfoliation and hydrogen exfoliation. In addition, a broadening of G band was observed in GO, G-S and G-H, and is attributed to an increase in the disorder of the samples.



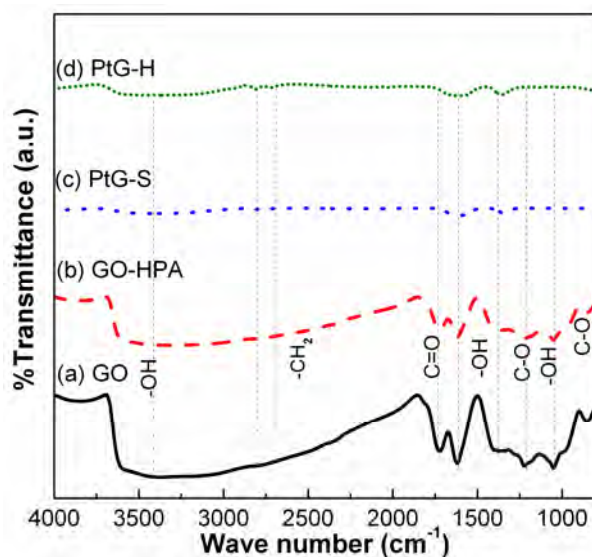
**Fig. S5.** Raman spectra of (a) Gr, (b) GO, (c) G-S and (d) G-H specimen.

**Table S2.** The  $I_D/I_G$  ratios tabulated for different samples determined from their corresponding Raman spectrum.

<b>Sample name</b>	<b><math>I_D/I_G</math></b>
Graphite	0
GO	0.97
GO-HPA	0.95
G-S	0.99
G-H	1.0
PtG-S	1.01
PtG-H	1.01

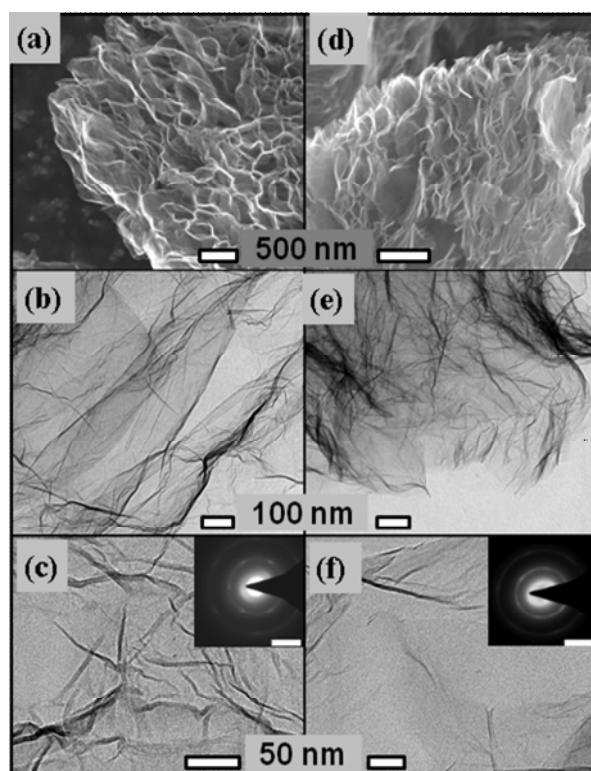


Fig. S6 (a) to (d) show the Fourier transform infrared spectroscopy (FT-IR) spectra of GO, GO-HPA, PtG-S and PtG-H respectively. The peaks at  $2803\text{ cm}^{-1}$  and  $2709\text{ cm}^{-1}$  correspond to symmetric and antisymmetric stretching vibrations of  $-\text{CH}_2$ .<sup>4</sup> In GO and GO-HPA, the highly broadened and intense peaks corresponding to the stretching vibrations  $-\text{OH}$  at  $3413\text{ cm}^{-1}$  and at  $1613\text{ cm}^{-1}$  indicate that the GO and GO-HPA samples contain large quantity of adsorbed water. Intense peaks corresponding to the  $\text{C}=\text{O}$  and  $\text{C}-\text{O}$  stretching vibrations of  $\text{COOH}$  groups at  $1730\text{ cm}^{-1}$  and  $1370\text{ cm}^{-1}$  are found in these samples.<sup>5</sup> These show GO and GO-HPA samples mainly consist of  $-\text{OH}$  and other oxygen containing functional groups. After exfoliation of GO-HPA with solar radiation at  $300\text{ }^\circ\text{C}$  and hydrogen at  $200\text{ }^\circ\text{C}$  the  $-\text{OH}$  functional groups are greatly reduced in intensity or are removed completely. The decrease in the intensities of the peaks at  $1730\text{ cm}^{-1}$ ,  $1370\text{ cm}^{-1}$  and  $1213\text{ cm}^{-1}$  corresponding to  $\text{C}=\text{O}$ ,  $\text{C}-\text{O}$  and  $-\text{OH}$  of  $-\text{COOH}$  groups reduce after hydrogen and solar exfoliation suggesting the partial removal of the these groups, in the form of water vapor and  $\text{CO}_2$ .<sup>6,7</sup>



**Fig. S6.** FTIR spectra of (a) GO, (b) GO-HPA, (c) PtG-S, and (d) PtG-H specimens.

Fig. S7 shows the FESEM and TEM images of G-S and G-H samples. The SEM images in S7 (a) and (d) show that GO has been homogeneously exfoliated via both the techniques. Fig. S7 (b and c) and (e and f) show the low- and high-magnification TEM images of G-S and G-H samples, respectively. The high magnification images confirm that both G-S and G-H have a wrinkled morphology. The insets in Fig. S7 (c) and (f) present the electron diffraction patterns for G-S and G-H, respectively. The brighter arcs are mainly due to the presence of large size crystallites of graphene sheets (4-5 layers stacked together along (002) plane as observed from XRD analysis) and the fainter rings are mainly because of the amorphous nature the G-S and G-H.



**Fig. S7.** The SEM (a,d), low-(b,e), and high-magnification (c,f) TEM images of G-S and G-H samples respectively. The insets in (c) and (f) show diffraction patterns with scale bars corresponding to  $5 \text{ nm}^{-1}$ .

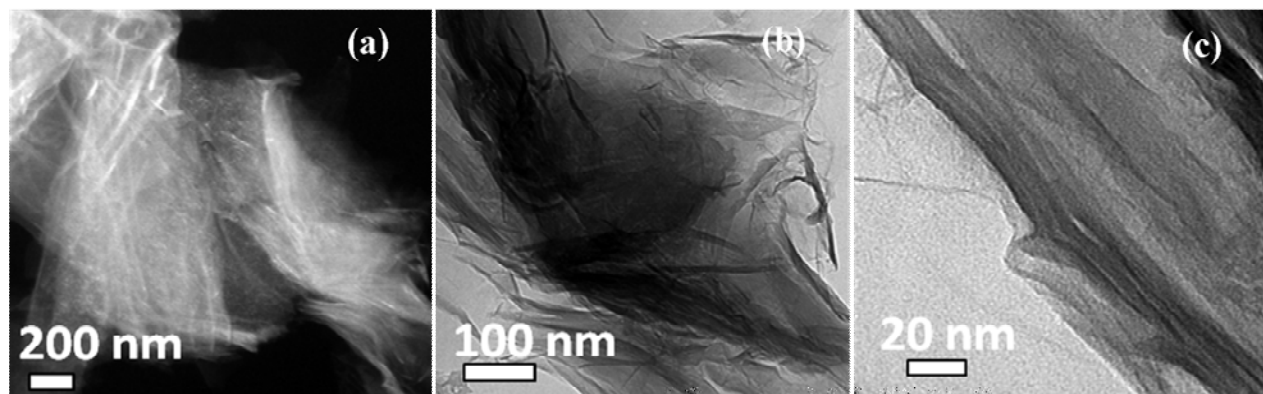


**Fig. S8.** (a) Dark field TEM image of GO-HPA, (b) Low-magnification and (c) high-magnification bright field TEM images of GO-HPA.

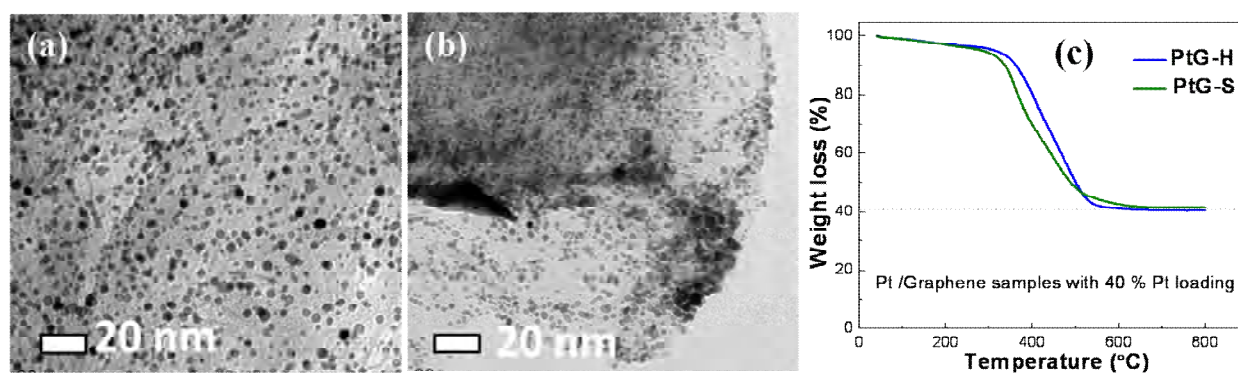


**Fig. S9.** TEM images of (a) PtG-S and (b) PtG-H samples for 40% Pt loading. (c) TGA of PtG-S and PtG-H samples for 40% Pt loading.

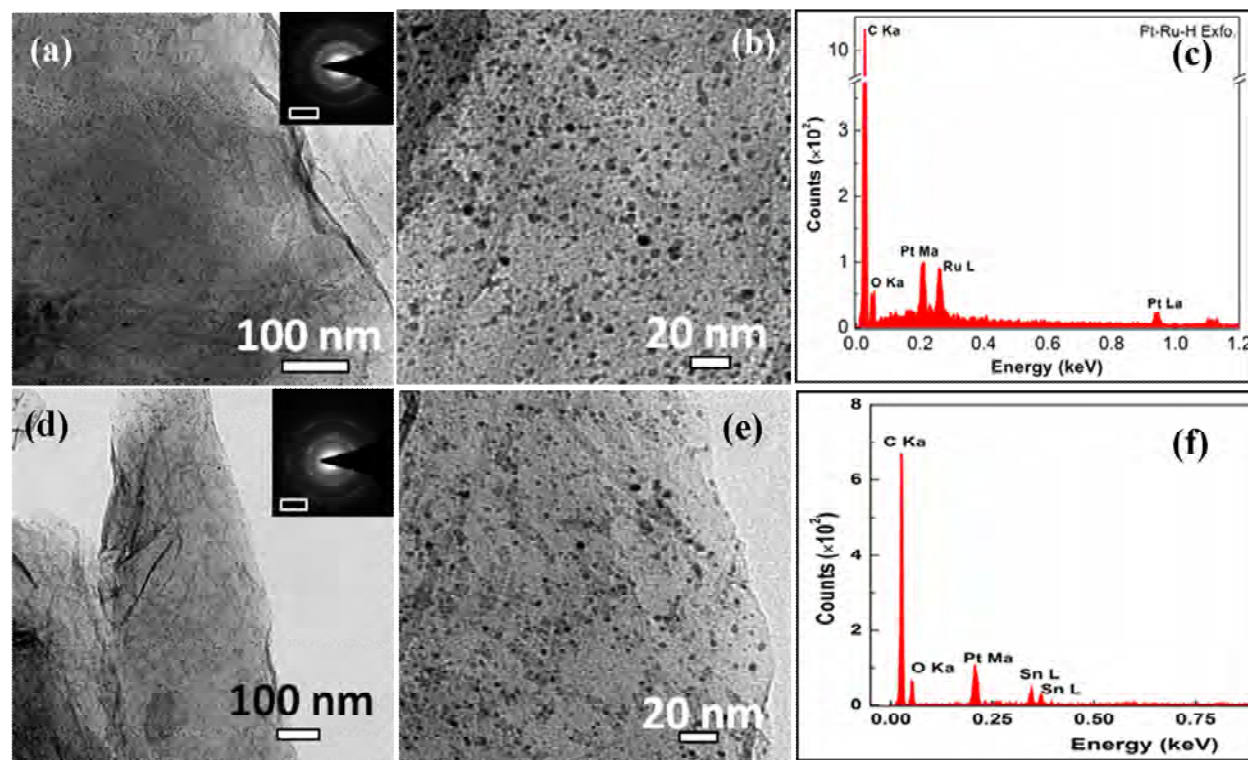


**Fig. S10.** Low and high-magnification TEM images and EDX of PtRu/graphene (Fig. S(a-c)) and PtSn/graphene (Fig. S(d-e)) synthesized by *in situ* hydrogen reduction. The insets in (a) and (d) show diffraction patterns with scale bars corresponding to  $5 \text{ nm}^{-1}$ .

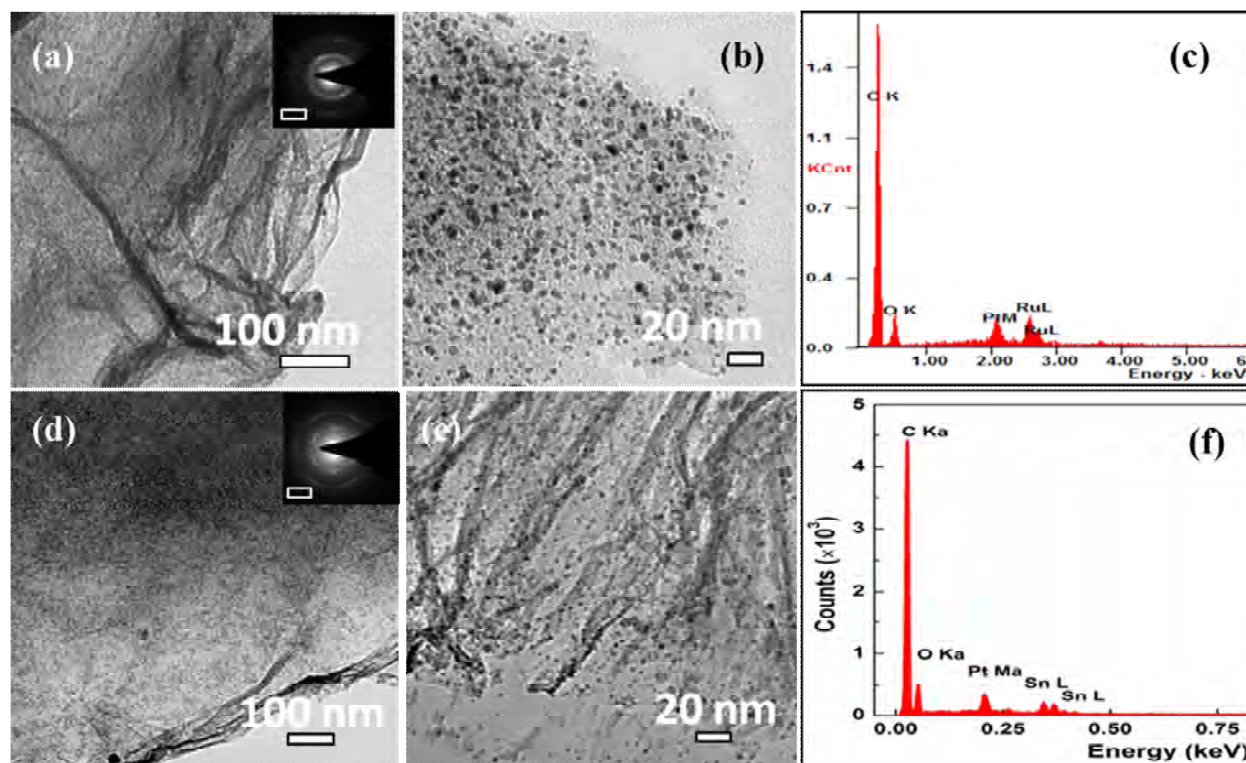


**Fig. S11.** Low and high-magnification TEM images and EDX of PtRu/graphene (Fig. S(a-c)) and PtSn/graphene (Fig. S(d-e)) synthesized by *in situ* solar reduction. The insets in (a) and (d) show diffraction patterns with scale bars corresponding to  $5 \text{ nm}^{-1}$ .

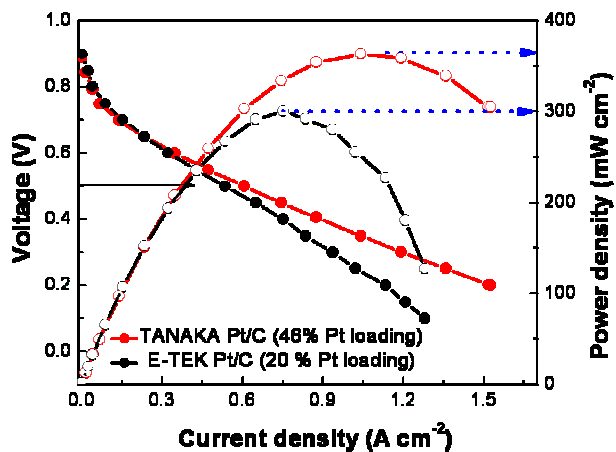


Fig. S12 : Polarization curve of TANAKA Pt/C (46% Pt loading) and E-TEK Pt/C (20% Pt loading) commercial electrocatalysts at 60°C.

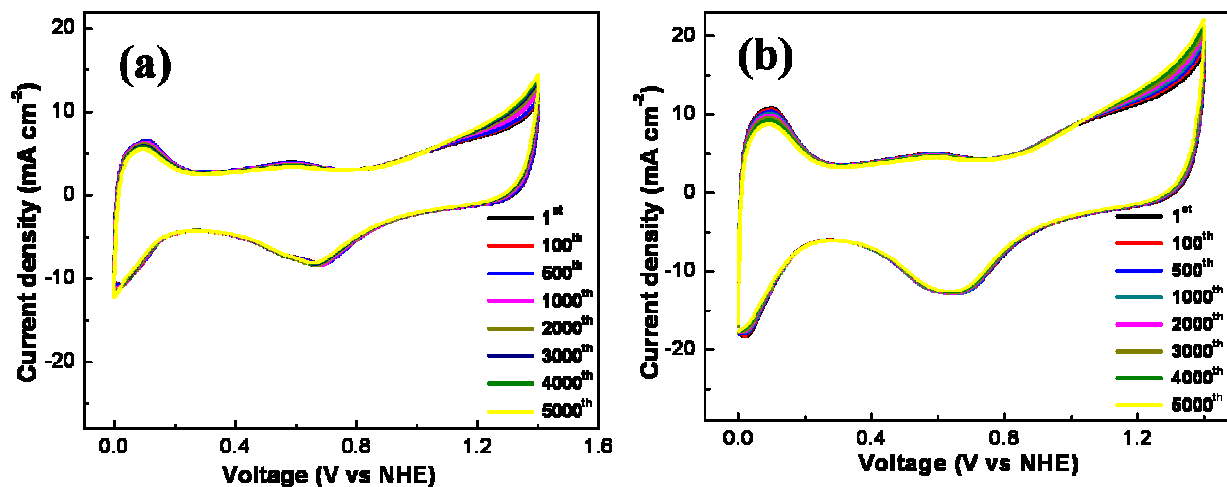


Fig. S13. Cyclic voltammetric stability studies of (a) PtG-S and (b) PtG-H samples for 5000 cycles at a scan rate of  $50\ mV\ sec^{-1}$ .

## References

1. A. E. Schweizer and G. T. Kerr, *Inorganic Chemistry*, 1978, **17**, 2326-2327.
2. H. K. Jeong, M. H. Jin, K. P. So, S. C. Lim and Y. H. Lee, *Journal of Physics D: Applied Physics*, 2009, **42**, 065418.
3. S. Reich and C. Thomsen, *Philosophical Transactions of the Royal Society of London. Series A: Mathematical, Physical and Engineering Sciences*, 2004, **362**, 2271-2288.
4. X. Sun, Z. Liu, K. Welsher, J. Robinson, A. Goodwin, S. Zaric and H. Dai, *Nano Research*, 2008, **1**, 203-212.
5. B. P. Vinayan, R. Nagar, K. Sethupathi and S. Ramaprabhu, *The Journal of Physical Chemistry C*, 2011, **115**, 15679-15685.
6. V. Eswaraiah, S. S. Jyothirmayee Aravind and S. Ramaprabhu, *Journal of Materials Chemistry*, 2011, **21**, 6800-6803.
7. A. Kaniyoor, T. T. Baby and S. Ramaprabhu, *Journal of Materials Chemistry*, 2010, **20**, 8467-8469.